CILAMCE 2017
Florianópolis - Santa Catarina - Brazil

WIND PRESSURE ANALYSIS ON NON-CONVENTIONAL STEEL STRUCTURES

Pedro Szloma Herr Zaterka

Cilmar Donizeti Basaglia

Mauricio Dario

João Alberto Venegas Requena

pedrozaterka@gmail.com

cbasaglia@fec.unicamp.br

mdario@terra.com.br

requena@fec.unicamp.br

Universidade Estadual de Campinas - UNICAMP

Cidade Universitria Zeferino Vaz - Barão Geraldo, 13083-970, Campinas, São Paulo, Brazil

Abstract. *As more complex numerical and analytical methods for structural engineering have grown more popular and accessible in the recent years, structures have become lighter and slender, which leads to a more optimized structural design but increases the significance of wind and other dynamic loads in the design. The importance of the correct wind load assumption is even more crucial in the case of steel structures, once they are much lighter than the concrete ones, thus more susceptible to pulling forces from wind action. This paper presents an unusual geometry, the Central Bus Station located in the city of Guarulhos, in the State of São Paulo, represented by its steel rooftop and adjacent buildings, comparing the wind tunnel results from the Institute for Technological Research - IPT with the results obtained using numerical modeling in the ANSYS CFX, with the element based finite volume method. The analysis seeks to use the data provided by the physical model as a benchmark to the numerical model, as it is a more renowned method, showing that the results are similar and the CFD can reliably provide the behavior of the fluid through the structure.*

Keywords: *Numerical Simulation, Wind Engineering, Computational Fluid Dynamics (CFD), Structural Modeling, Steel Structures*

1 INTRODUCTION

Wind effects on structures are a matter of concerning that has been constantly rising in the past years. The correct assumption of the wind loads in the design phase of a building can be the difference between a light, cheap and well designed structure and a heavier, expensive or non-optimal, and even in critical cases, unsafe.

Currently there are two main ways of estimating the wind loads: The national codes (Such as the ABNT NBR6123/1988 from Brazil or the Eurocode from Europe) that provide guidelines for this calculation based on geometrical features and statistic factors. This guidelines can be useful and trustworthy for more usual geometries such as gable rooftops or rectangular buildings as a general method for obtaining wind pressure but cannot be used for every particular architecture.

For cases where the shape of the building cannot be satisfactorily contemplated by the codes the usual method is the wind tunnel, where a scaled model of the building and its surroundings is built and submitted to wind flows that would impact the real structure. However this method, even being more precise, has some drawbacks as it is as very expensive and time demanding method, as well as subjected to considerable variations depending on the scale or the tunnel itself, as showed by Robertson & Moran (1986).

With the advance in computational capability and numerical methods a new option is arising as an alternative to the wind tunnel, the computational fluid dynamics (CFD) analysis. Largely used in other fields such as chemical engineering and mechanical engineering, this method can represent through computational analysis with the finite volume method how the wind behaves when meeting the building.

This interaction between fluid and structure obtained in the analysis can provide the same pressure results as the wind tunnel with the advantage of being faster, cheaper and needing a smaller structure to perform the analysis.

Concerning the reliability of this new method, as Blocken et al (2007) and Bourdin & Wilson (2008) studied, the parameters used in the model and the boundary conditions are of major importance in obtaining good results. Comparative studies of ships and isolated rooftops were carried on by Janssen et al (2017) and del Coz Díaz et al(2009) respectively who obtained reliable results for such cases.

The CFD analysis have also other benefits as it can perform a thermal comfort analysis parallel with the wind pressure, as done by van Hoof & Bloken (2010) obtaining results close to in site measures. For this study, there will only be used the pressure and wind velocity results from the numerical model as they will be compared with a wind tunnel experiment in which these were the variables measured.

This paper seeks to compare the results from the experiment done by the Institute for Technological Research (IPT) of the Guarulhos Bus Station with a computational analysis modeled in the CFD software ANSYS CFX. This will allow a comparison of a non-conventional structure with surrounding buildings that affect the wind flow through the station and how it affects the rooftop in terms of pressure. As this is a work in progress there will be presented two angles of incidence of wind acting on the structure, in future work more angles will be analyzed.

2 CASE OF STUDY

For this paper it was done a comparative study of a real building, having the wind tunnel results, these were used as benchmark for the numerical analysis.

2.1 The Structure

The structure used as the case of study in this paper is the Central Bus Station of Guarulhos (seen in Fig. 1). Located in the city of Guarulhos, in the state of São Paulo, as the terminal is in middle of the city, the roughness length considered (z_0) was 0.13 m, as it was the same in both physical and computational models.

Figure 1: Satellite picture of the structure and surrounding buildings (Source: Google Earth)

The structure is composed by the steel rooftop and side wings, as well as beams and columns. The cables were not considered due to its small influence in the wind behavior through the structure as well as the fact that this feature increases the mesh density by a considerable amount. Also, there were added surrounding and internal buildings, as these have an influence in the wind flow that cannot be ignored.

The dimensions of the rooftop were based in the construction project and in situ measurements, and the surrounding and internal buildings had their dimensions determined by satellite photos. The determination of said dimensions were done independently for the physical and computational models.

2.2 Wind Tunnel

The wind tunnel analysis was carried out by the Instituto de Pesquisas Tecnolgicas IPT, using the Wind Tunnel for Atmospheric Boundary Layer.

The model was done in a scale 1:100 keeping the geometric similarities.

3 COMPUTATIONAL MODELLING

For the computational analysis, it was carried out using ANSYS 18 CFX, which uses the element-based finite volume method to describe how the wind behaves when in contact with the structure. The model used was the Reynolds-Averaged Navier Stokes (RANS), for it provide satisfactory results for the pressure analysis at a much smaller computational effort as other options such as the Direct Numerical Simulation (DNS) and the Large Eddy Simulation (LES) offer more precise results but at much larger computational demand.

For the turbulence model, the model chosen was the k-ε, as used by Blocken et al (2006), Yin et al (2009),van Hoof & Bloken (2010), Janssen (2017) and other authors along the years. Being a model which presents satisfactory results and can work with higher Y+ values comparing to other CFX models, like SST and k-ω, that can work only with smaller values requiring a much denser mesh to work properly, and consequently a considerable increase in the computational cost of the analysis.

As the standard k-ε model does not represent correctly some parts of the behavior the wind-structure interaction, Franke et al (2007) recommends the use of an improved k-ε model. For the availability in CFX and the advantage of being less computationally demanding than the realizable model, the turbulence model used was the RNG k-ε as used by Gomes et al (2005).

3.1 Geometry Representation

The geometry was represented as the rooftop, adjacent buildings and inner buildings, but some simplifications were made as some details would not have great impact in the wind pressure on the structure but would have a considerable increase in the mesh statistics. Apart from the cables the trusses were approximated as a continuous thickness equivalent to the trusses' high. Different views of the geometry representation in the computational model are shown in Fig. 2.

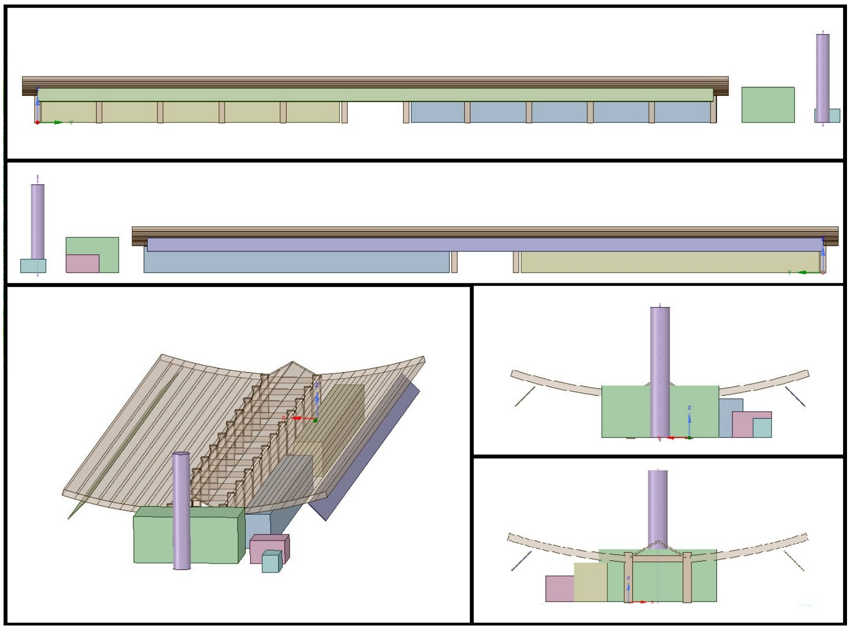

Figure 2: Different views from the modelled geometry

The upper view can be seen in Fig. 3, with the wind directions addressed in this paper assigned (0° and 90°).

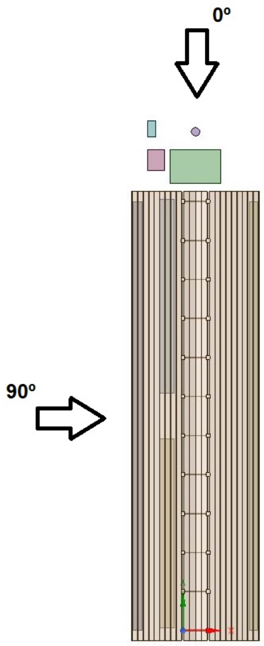

Figure 3: Upper view of the structure and adjacent buildings on ANSYS with wind incidence

For the 90° incidence the surrounding circular building and the smaller rectangular one were not considered as they would not affect the wind pressure on the structure but increase the mesh refinement needed.

3.2 Mesh Generation

The mesh was generated inside the Fluent meshing present in ANSYS 18 Workbench. The domain was discretized in tetrahedral elements with the inflation estimated for a Y+ of 200 on the structure surface and adjacent buildings. The domain in which it is generated respects both ANSYS and Franke et al (2004) recommendations regarding the position of the boundaries. The mesh quality was evaluated based on skewness ($\leq$0.9), orthogonal quality ($\geq$0.15) and aspect ratio ($\leq$100, with exceptions for the boundary layer) of the elements, the values adopted being the recommended from the software developer. The resulting mesh can be seen in Fig. 4.

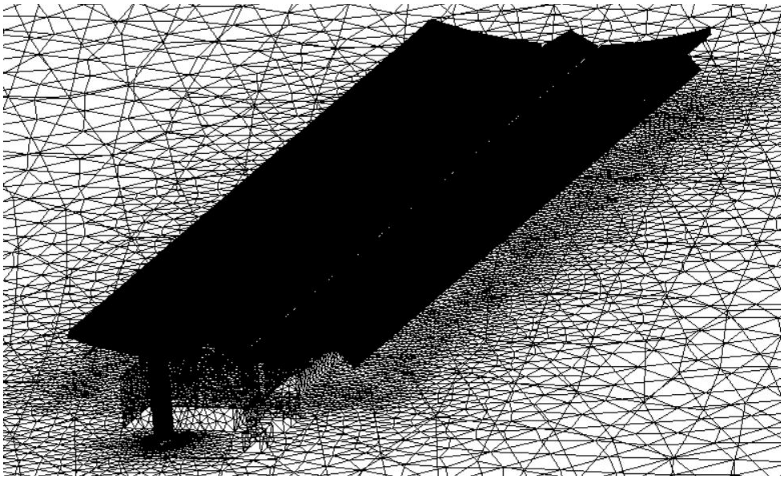

Figure 4: Resulting mesh in the structure region

The resulting mesh contains 14,795,680 nodes and 9,469,016 elements for the $0°$ analysis and 20,654,728 nodes and 13,285,466 elements for the $90°$ analysis, the difference resulting from the fact that the domain for the $90°$ had to be larger in order to respect the minimum dimensions adopted. The statistics for each quality criteria can be seen in Table 1:

Table 1: Mesh quality parameters

	Wind at $0°$		Wind at $90°$	
Parameter	Average	Standard Deviation	Average	Standard Deviation
Skewness	0.246	0.128	0.242	0.139
Orthogonal Quality	0.832	0.158	0.832	0.160
Aspect Ratio	14.877	37.001	18.987	45.621

3.3 Boundary Conditions

The velocity profile on the inlet used was the logarithmic, represented in Eq. (1), with the characteristic velocity (v_k) equal 35.7 m/s as used in the physical experiment for it is the velocity in the region according to the statistical and usage factors presented in the Brazilian Code ABNT NBR6123/1988.

$$v(z) = v_k \frac{u^*}{K} ln(\frac{z - z_0}{z_0}). \tag{1}$$

Where z_0 is the roughness length and z is the vertical coordinate from the ground. The friction factor u^* divided by the Von-Karmann constant (K = 0.42) is given by the Eurocode equation showed in Eq. (2).

$$\frac{u^*}{K} = 0.234 {z_0}^{0.07}. \tag{2}$$

For the turbulence parameters of the *k*-ε (*k* being the kinectic energy and ε the turbulent dissipation) on the inlet, Franke et al (2007) recommends the formulation stated by Richards

& Hoxey (1993) for the adequate modeling of the atmospheric surface layer of steady RANS analysis. They can be seen in Eq. (3) and Eq. (4).

$$k = \frac{u^{*2}}{\sqrt{C_\mu}}. \quad (3)$$

$$\varepsilon = \frac{u^*}{K(z + z_0)}. \quad (4)$$

Where C_μ is a model constant of the standard k-ε model.

The analysis was carried out as a steady state analysis, based on the works of Van Hooffe et al (2011), Montazeri & Blocken (2013) and Janssen et al (2017). Regards of, once the wind tunnel had 60 seconds of wind, which can be considered as a steady state flow, as well as it would be a considerable time for a transient analysis.

4 RESULTS AND DISCUSSION

The analysis was performed for two wind incidences, $0°$ and $90°$ as indicated in Figure 3. The side names at $0°$ are indicated as right and left as the structure is seen from direct were the wind comes. For the wind at $90°$ the sides are indicated as upwind and downwind referring to the wind stream across the structure.

The data provided by IPT was in the form of the ΔCP, which is the difference between the pressure coefficient in the external(CP_e) and internal faces(CP_i). The results were given in contours, the ones used in this analysis, 0 and 90 degrees are seen in Fig. 5 and Fig. 6.

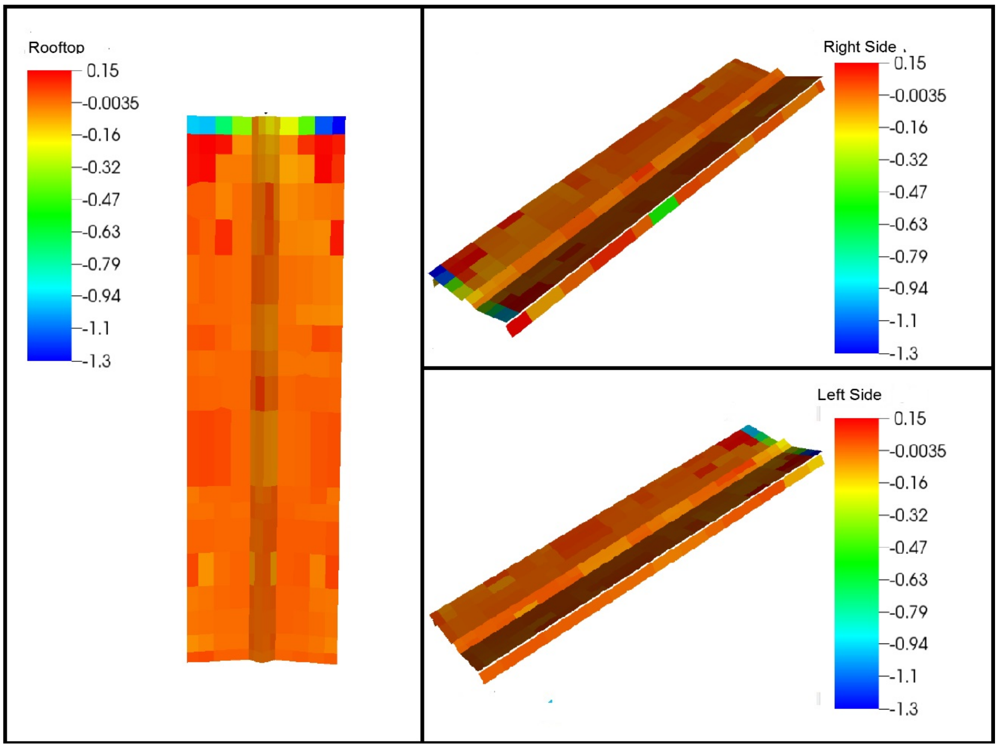

Figure 5: ΔCP values provided by the wind tunnel with wind at $0°$

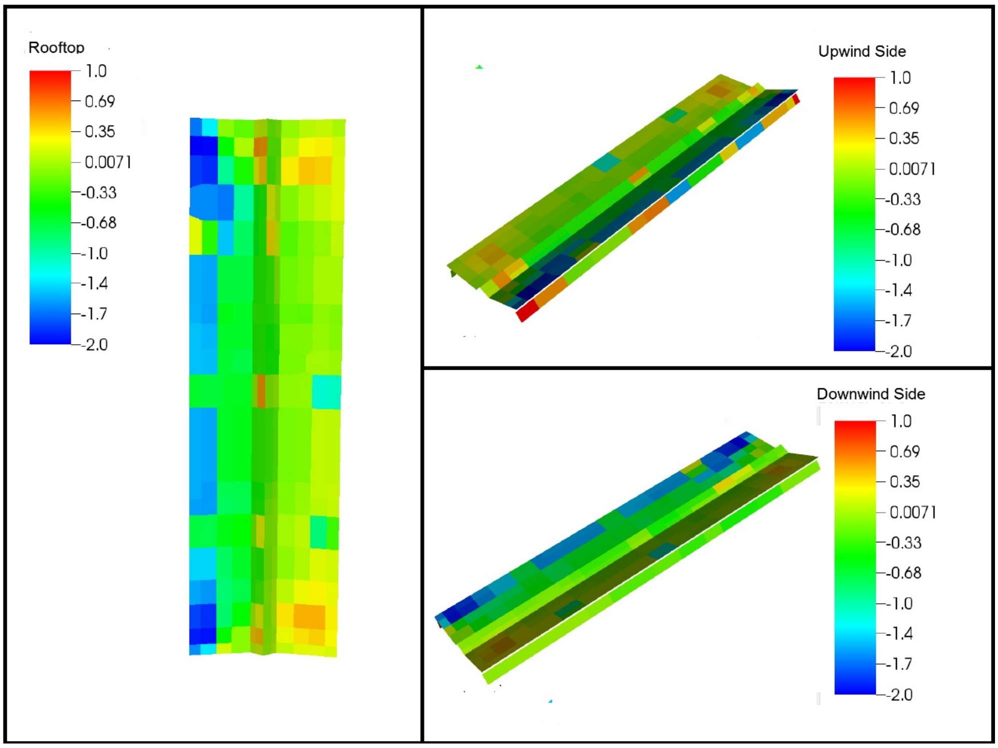

Figure 6: ΔCP values provided by the wind tunnel with wind at $90°$

For the CFD results, this coefficients are calculated from the obtained pressure acting on the surface. The expression used is shown in Eq. 5 and it is used to calculate both external and internal pressure coefficients.

$$CP = \frac{p - p_{ref}}{\frac{1}{2}\rho {v_k}^2}. \tag{5}$$

Where p is the pressure on the surface, p_{ref} is the pressure of the free stream, ρ is the air density and v_k is the reference velocity (35.7 m/s).

While CFX does not permit the operation of subtracting the coefficients from one face to the other, it can provide the separated contours of both CP_e (Fig. 7 and Fig. 9) and CP_i (Fig. 8 and Fig. 10). The wind behavior can be observed as well as high gradient zones that are not shown in the physical experiment results.

Even without subtracting the values, high concentration gradients can be observed in the structure and critical areas can already be estimated. The interference of inner buildings is evident seeing the internal coefficients, where there is an increase in pressure on the areas preceding those buildings, showing that the air goes up and backwards after hitting their faces.

For a better understanding on how the wind behaves around the main structure and surrounding buildings, the streamline is show in various views in Fig. 11 and 12.

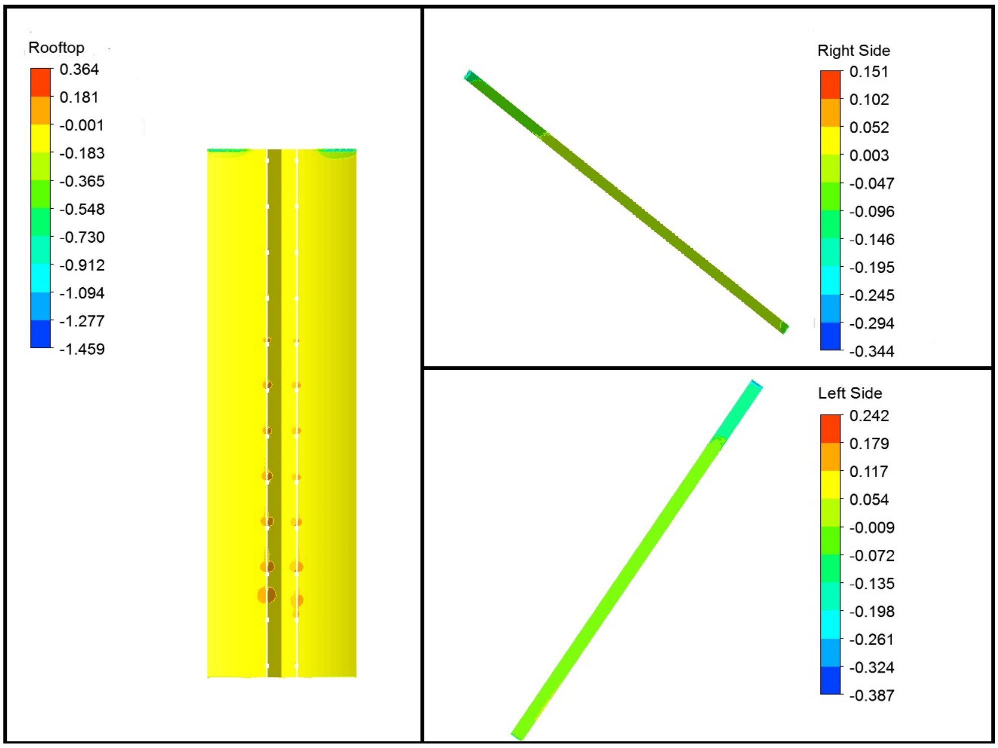

Figure 7: CP$_e$ from the CFD analysis with wind at 0°

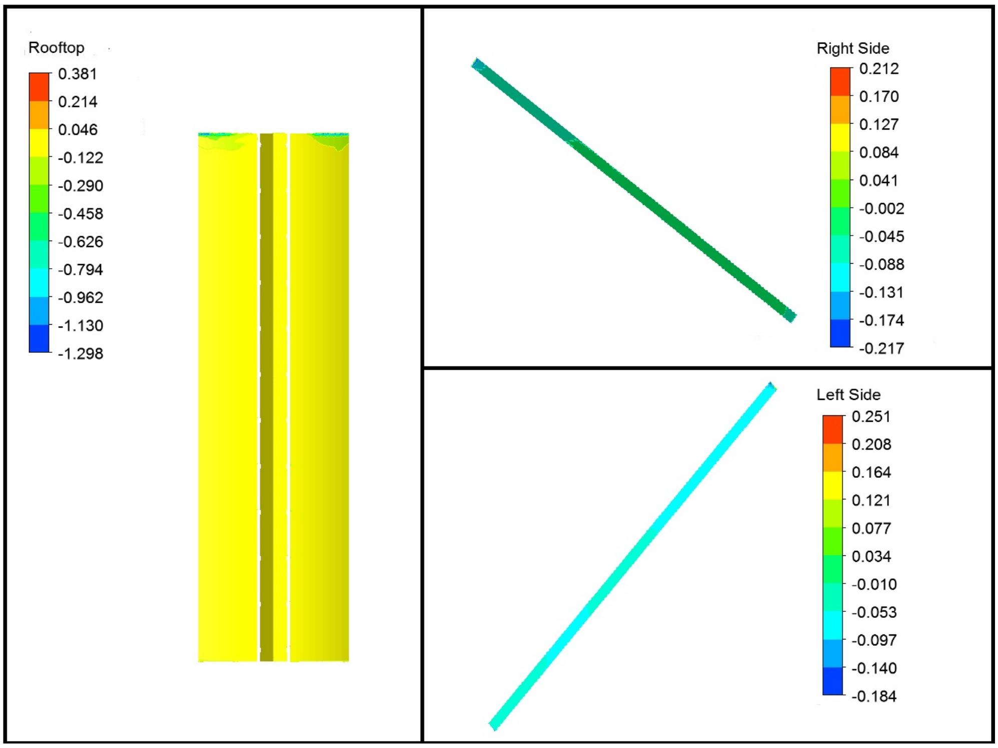

Figure 8: CP$_i$ from the CFD analysis with wind at 0°

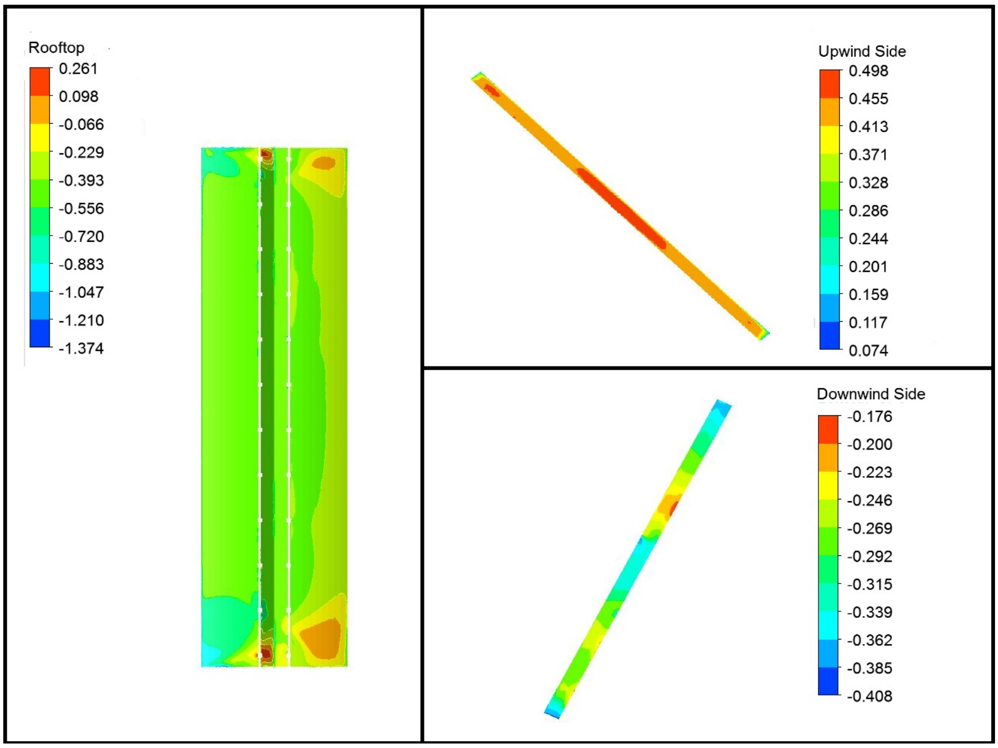

Figure 9: CP$_e$ from the CFD analysis with wind at $90°$

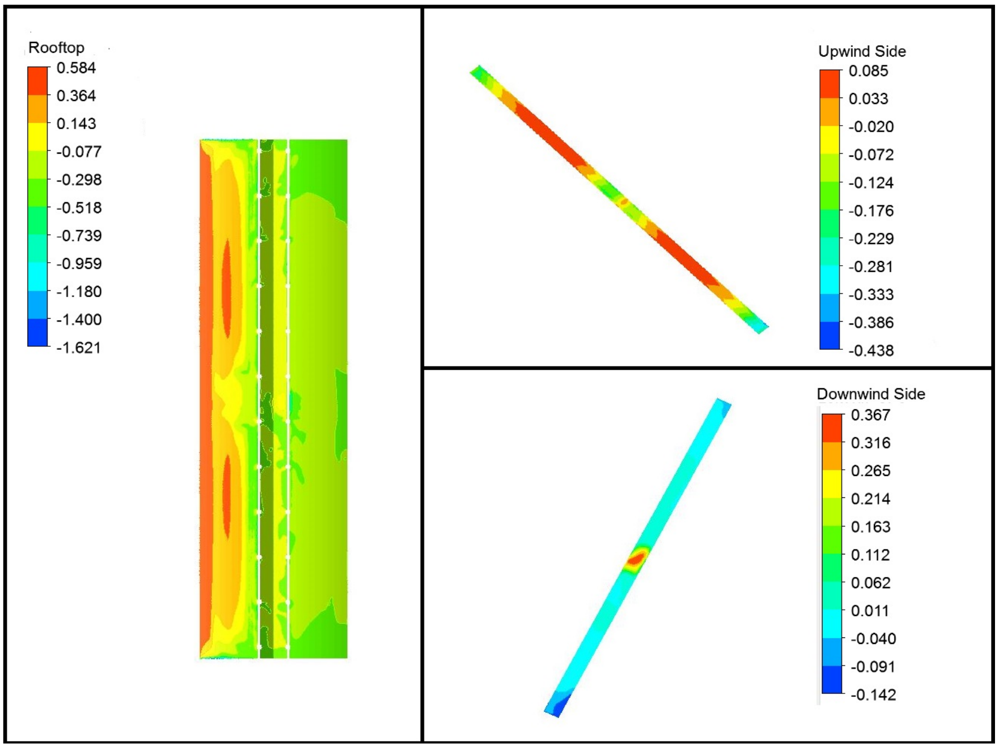

Figure 10: CP$_i$ from the CFD analysis with wind at $90°$

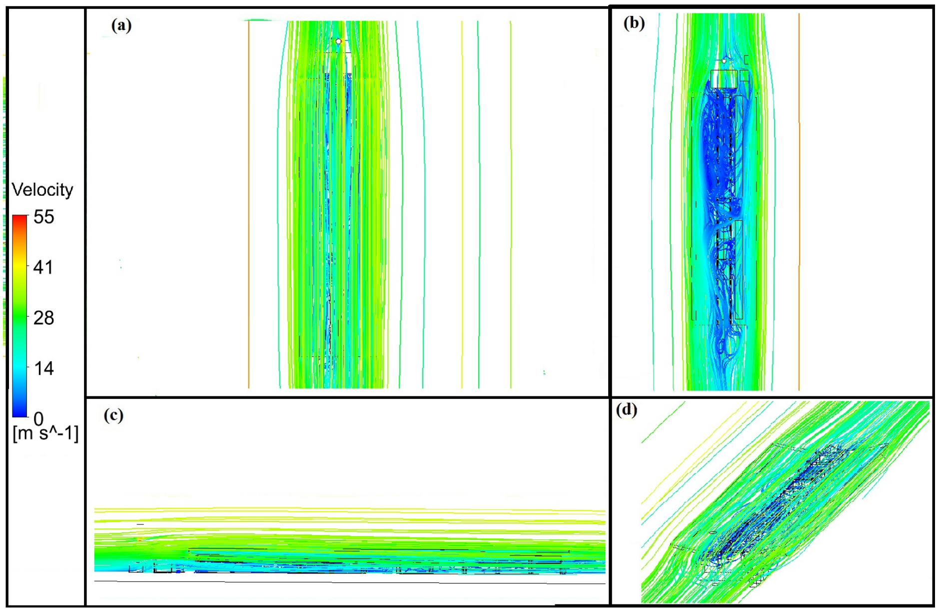

Figure 11: Wind velocity surrounding the building with wind at $0°$: (a) Upper view; (b) Lower view; (c) Side view; (d) Perspective view

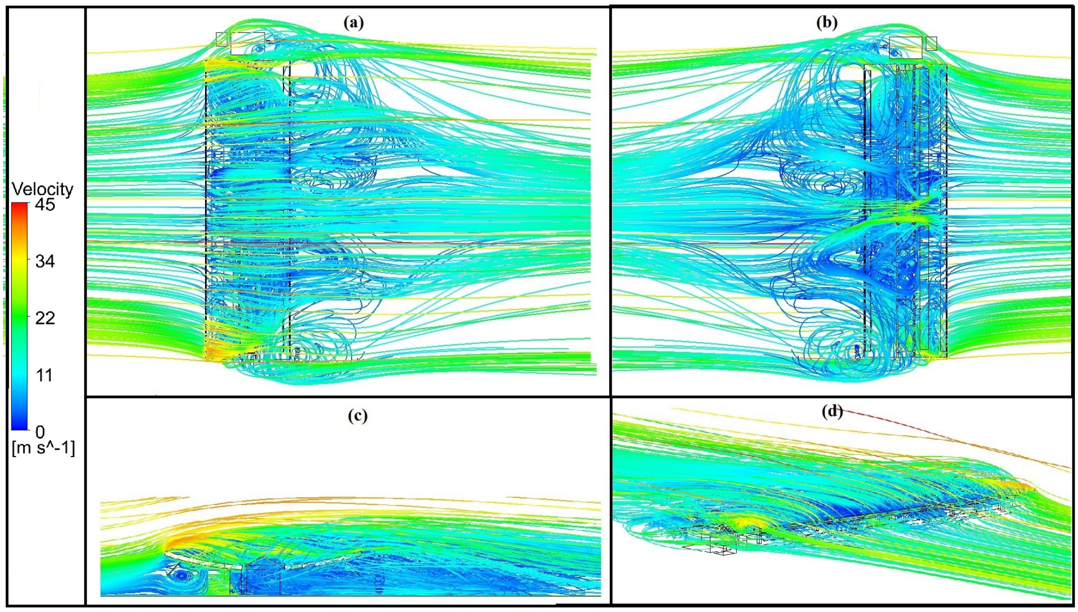

Figure 12: Wind velocity surrounding the building with wind $90°$: (a) Upper view; (b) Lower view; (c) Side View; (d) Perspective view

For the $0°$ there can be seen the influence of the surrounding buildings that serve as a block for part of the wind stream. The velocity inside the Bus Terminal has lower values comparing to the velocity outside and the formation of vortices is not clearly seen.

High pressure coefficients are observed in the area close to the front of the rooftop (Where the wind first collides with the surface) and near the columns, as for most of the building these coefficients present a considerably small value.

In the $90°$, it is observed the formation of vortices and the increase of wind velocities in the turbulent parts of the upwind faces. The inner buildings work as a barrier blocking the wind generating lower velocities inside the bus terminal. Except in the area between those buildings, where a considerable increase in the stream velocity is noted.

For a more quantitative analysis the structure was divided in areas as present in the wind tunnel report (The areas are shown in Fig. 13).

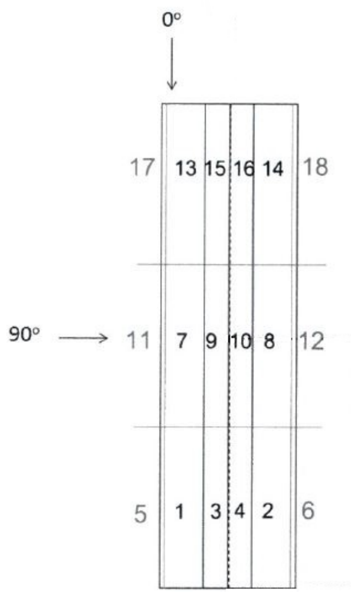

Figure 13: Area number of the structure results

The wind tunnel result was provided divided in this areas, so to compare these coefficients the data from the model were exported and the average pressure coefficient was calculated for the same areas. With this averages it was possible to find ΔCP = CP_e-CP_i for the numerical model.

This allowed a direct comparison with results from both physical and numerical methods. The ΔCP from both methods as well as their difference is shown in Table 2.

A further comparison is done with the average pressure coefficient from the whole structure, with the average value from the areas in which the building was previously divided. The values for each average, their difference in value and percentage can be seen in Tables 2 and 3.

Table 2: Pressure coefficients for wind at $0°$

Area	Wind Tunnel	CFD	Difference
1	0.00	0.00	0.00
2	0.02	0.02	0.00
3	0.00	0.01	0.01
4	0.01	0.02	-0.01
5	-0.03	0.00	-0.03
6	0.01	0.02	-0.01
7	0.03	0.01	0.02
8	0.01	0.02	-0.01
9	-0.02	0.03	-0.05
10	-0.05	0.02	-0.07
11	-0.01	0.01	-0.02
12	-0.02	0.01	-0.03
13	-0.05	-0.08	0.03
14	-0.07	-0.09	0.02
15	-0.03	-0.08	0.05
16	-0.06	-0.09	0.05
17	-0.02	0.00	-0.02
18	-0.07	0.00	-0.07

Table 3: Pressure coefficients for wind at $90°$

Area	Wind Tunnel	CFD	Difference
1	-1.05	-0.65	-0.40
2	0.14	0.01	0.13
3	-0.22	-0.15	-0.07
4	-0.09	-0.15	0.06
5	0.41	0.17	0.24
6	-0.03	0.03	0.06
7	-1.02	-0.59	-0.43
8	-0.06	-0.12	0.06
9	-0.38	-0.18	0.20
10	-0.38	-0.15	-0.23
11	0.77	0.20	0.57
12	-0.24	-0.08	-0.16
13	-1.06	-0.64	-0.42
14	0.08	-0.04	0.12
15	-0.10	-0.19	0.09
16	-0.22	-0.17	0.05
17	0.54	0.14	0.40
18	-0.14	0.00	-0.14

Table 4: Average pressure coefficients

Average ΔCP	Wind Tunnel	CFD	Total Difference
$0°$	-0.02	-0.01	-0.01
$90°$	-0.17	-0.14	-0.03

For the critical value on the structure, the physical model has a minimum ΔCP value of -1.3 for 0° and -2.0 for 90°, while in the CFD analysis the critical point found has a ΔCP of -1.45 and -2.13 for each case respectively, therefore for this case the value differs by 0.15 and 0.13, as seen in Table 5.

Table 5: Critical pressure coefficients

Critical ΔCP	Wind Tunnel	CFD	Total Difference	Percentage Difference
0°	-1.3	-1.45	-0.15	11.5
90°	-2.00	-2.13	-0.13	6.5

The results of the absolute average pressure coefficient and the critical value showed close results, the average of the CFD analysis being greater than the wind tunnel analysis whereas the critical value present in the computational analysis results in a higher suction pressure on the structure.

Analyzing Table 2 a considerable difference can be noted in some of the areas. Looking at Figure 5 and comparing it to figures 7 and 8 it is seen that some variations in the surface pressure are present in the numerical model. With that, the high gradient areas may have contributed to this discrepancy, affecting the area average.

Other than that, the simplifications in the geometry may present a key factor in the divergence between the results, as the original structure has been changed in different ways in both analysis in order to suit each method better.

5 CONCLUSIONS

In this study, a Computational Fluid Dynamics (CFD) analysis was compared with a wind tunnel experiment performed in the non-conventional geometry of the Guarulhos Bus Terminal. With the representation of the surrounding buildings and some simplifications in the geometry, a RANS model was used to perform the analysis in two incidences of wind, 0° and 90°.

As for the results, the average value of the divided areas is closer in the 0° case, as it is observed a less turbulent behavior of the fluid in the interaction with the structure and a more uniform distribution of the pressure coefficients along the rooftop. Higher pressure values are seen in the area on the upstream part, where the formation of vortices is noted, this occurrence is present also in the physical experiment, where the high ΔCP values are also observed.

The streamline plot shows the how the surrounding buildings influence the wind behavior around the structure. The outside building acting as a blockage for the fluid, making it achieve lower velocities in the inside.

The 90° analysis presented a greater formation of vortices, and higher pressure coefficients, as the wind blows directly in the structure, not having surrounding building upstream. The presence of the inner buildings and side buildings created zones of higher pressure concentration of the lower faces of the rooftop, these zones resulting in a larger divergence with the wind tunnel results.

But with the average pressure on the whole structure and the critical values the result comes much closer, with a 17.64% difference in the whole average and the CFD analysis having a critical value 6.5% higher than the wind tunnel model. When comparing the contours the distribution of the coefficients are consistent on both analysis, the computational one presenting different values in the geometry discontinuities and close to the inner buildings.

The streamline for the 90° case showed how the inner buildings act as a blockage for the flow inside most of the terminal, but generating a higher velocity region in the gap between these buildings, forming a Venturini effect. This effects results can be seen in the CP_i values on the downstream region of the surface, where a high pressure region is observed.

The computational model, performed on the finite volume software ANSYS CFX 18, had some discrepancy with the benchmark proposed, despite reaching close critical values, this shows that the parameters can be improved and should be checked in order to find the possible sources of this discrepancy between the more renowned method and the computational analysis. As this is a research in progress, for future development, changes in the parameters and conditions adopted, as well as more wind incidences will be compared to ensure the parameters adopted offer a reliable result for all cases, and the identification of the critical wind direction and the comparison with the experimental data.

ACKNOWLEDGEMENTS

The authors would like to thank the *Guarulhos city council* for the support allowing the use of the data from the wind tunnel, *IPT - Institute for Technological Research* for providing said data, and the *CAPES - Coordination for the Improvement of Higher Education Personnel* and the *CNPq - National Council for Scientific and Technological Development* for funding this research.

REFERENCES

Ansys, C.F.X., 2017. Solver theory guide. *Ansys CFX Release*, 18.

Blocken, B., Stathopoulos, T. & Carmeliet, J., 2007. CFD simulation of the atmospheric boundary layer: wall function problems. *Atmospheric environment*, 41(2), pp.238-252.

Bourdin, P., & Wilson, J. D., 2008. Windbreak aerodynamics: is computational fluid dynamics reliable?. *Boundary-Layer Meteorology*, 126(2), pp. 181-208.

CEN., 2007. Eurocode 1: Actions on structures - Part 1-4:General actions-Wind actions.

del Coz Díaz, J.J., Nieto, P.G., Prez, J.G. and Navarro, A.M., 2009. Numerical analysis of the pressure field on curved and open self-weighted metallic roofs due to the wind effect by the finite volume method. *Applied Mathematics and Computation*, 209(1), pp.31-41.

Franke, J., Hellsten, A., Schlnzen, H., & Carissimo, B., 2007. Best Practice Guideline for the CFD Simulation of Flows in the Urban Environment. *COST Action 732: Quality Assurance and Improvement of Microscale Meteorological Models* .

Franke, J., Hirsch, C., Jensen, A.G., Krs, H.W., Schatzmann, M., Westbury, P.S., Miles, S.D., Wisse, J.A. and Wright, N.G., 2004. Recommendations on the use of CFD in wind engineering. *Cost action* C (Vol. 14, pp. C1).

Gomes, M.G., Rodrigues, A.M. & Mendes, P., 2005. Experimental and numerical study of wind pressures on irregular-plan shapes. *Journal of Wind Engineering and Industrial Aerodynamics*, 93(10), pp.741-756.

Janssen, W. D., Blocken, B. & van Wijhe, 2017. H. J. CFD simulations of wind loads on a container ship: Validation and impact of geometrical simplifications. *Journal of Wind Engineering and Industrial Aerodynamics*, v. 166, pp. 106-116.

Montazeri, H. & Blocken, B., 2013. CFD simulation of wind-induced pressure coefficients on buildings with and without balconies: validation and sensitivity analysis. *Building and Environment*, 60, pp.137-149.

NBR6123, A.B.N.T., 1988. Wind loads in buildings. *ABNT-Brazilian Association of Technical Codes*, Rio de Janeiro (in Portuguese).

Richards, P.J. & Hoxey, R.P., 1993. Appropriate boundary conditions for computational wind engineering models using the k-ϵ turbulence model. *Journal of wind engineering and industrial aerodynamics*, 46, pp.145-153.

Robertson, A.P. & Moran, P., 1986. Comparisons of full-scale and wind-tunnel measurements of wind loads on a free-standing canopy roof structure. *Journal of Wind Engineering and Industrial Aerodynamics*, 23, pp.113-125.

Stathopoulos, T., 1997. Computational wind engineering: Past achievements and future challenges. *Journal of Wind Engineering and Industrial Aerodynamics*, 67, pp.509-532.

Van Hooff, T. & Blocken, B., 2010. Coupled urban wind flow and indoor natural ventilation modelling on a high-resolution grid: A case study for the Amsterdam ArenA stadium. *Environmental Modelling & Software*, 25(1), pp.51-65.

Van Hooff, T., Blocken, B., Aanen, L. & Bronsema, B., 2011. A venturi-shaped roof for wind-induced natural ventilation of buildings: wind tunnel and CFD evaluation of different design configurations. *Building and Environment*, 46(9), pp.1797-1807.

Yin, Y., Zhang, T., Han, Q. & Yang, H., 2009. Determination of wind pressure coefficients for arc-shaped canopy roof with numerical wind tunnel method. *Transactions of Tianjin University*, 15(5), pp.360-365.